



Tetracosahexaenoylethanolamide, a novel *N*-acylethanolamide, is elevated in ischemia and increases neuronal output

Lin Lin^{1,†}, Adam H. Metherel^{1,†,*}, Mathieu Di Miceli², Zhen Liu¹, Cigdem Sahin³, Xavier Fioramonti², Carolyn L. Cummins³, Sophie Layé², and Richard P. Bazinet¹

¹Department of Nutritional Sciences, Faculty of Medicine, University of Toronto, Toronto, Ontario, Canada, ²Université de Bordeaux, INRA, Bordeaux INP, NutriNeuro, UMR 1286, Bordeaux, France, and ³Department of Pharmaceutical Sciences, University of Toronto, Toronto, Ontario, Canada

Abstract *N*-acylethanolamines (NAEs) are endogenous lipid-signaling molecules derived from fatty acids that regulate numerous biological functions, including in the brain. Interestingly, NAEs are elevated in the absence of fatty acid amide hydrolase (FAAH) and following CO₂-induced ischemia/hypercapnia, suggesting a neuroprotective response. Tetracosahexaenoic acid (THA) is a product and precursor to DHA; however, the NAE product, tetracosahexaenoylethanolamide (THEA), has never been reported. Presently, THEA was chemically synthesized as an authentic standard to confirm THEA presence in biological tissues. Whole brains were collected and analyzed for unesterified THA, total THA, and THEA in wild-type and FAAH-KO mice that were euthanized by either head-focused microwave fixation, CO₂ + microwave, or CO₂ only. PPAR activity by transient transfection assay and ex vivo neuronal output in medium spiny neurons (MSNs) of the nucleus accumbens by patch clamp electrophysiology were determined following THEA exposure. THEA in the wild-type mice was nearly doubled ($P < 0.05$) following ischemia/hypercapnia (CO₂ euthanization) and up to 12 times higher ($P < 0.001$) in the FAAH-KO compared with wild-type. THEA did not increase ($P > 0.05$) transcriptional activity of PPARs relative to control, but 100 nM of THEA increased ($P < 0.001$) neuronal output in MSNs of the nucleus accumbens. Here we identify a novel NAE, THEA, in the brain that is elevated upon ischemia/hypercapnia and by KO of the FAAH enzyme. While THEA did not activate PPAR, it augmented the excitability of MSNs in the nucleus accumbens. Overall, our results suggest that THEA is a novel NAE that is produced in the brain upon ischemia/hypercapnia and regulates neuronal excitation.

Supplementary key words tetracosahexaenoic acid • fatty acid amide hydrolase • patch clamp • neurons • brain lipids • fatty acid • fatty acid/metabolism • peroxisome proliferator-activated receptors • fatty acid amide hydrolase-knockout

N-acylethanolamines (NAEs or fatty acid ethanolamines) are lipid-signaling molecules that play decisive roles in

multiple physiological pathways. NAEs are synthesized in vivo from respective fatty acid precursors, with the subsequent breakdown of NAEs to unesterified fatty acids occurring via fatty acid amide hydrolase (FAAH) (1, 2). NAEs exhibit a wide range of biological functions. For instance, arachidonoylethanolamide (AEA or anandamide) is a PUFA-derived endocannabinoid that regulates fear (1), anxiety (3), pain sensation (4), energy balance, appetite, memory (5), sedation, and euphoria (6). AEA modulates dopamine levels in the nucleus accumbens (7, 8), a brain region of the striatum involved in reward processes (9). Moreover, inhibition of FAAH, the enzyme responsible for AEA degradation, enhances AEA-induced dopamine release in the nucleus accumbens of rats (8). Medium spiny neurons (MSNs) represent the major neuronal population within the nucleus accumbens (10) and control a wide array of functions, such as habit, motor control, reward, and motivation.

Docosahexaenoylethanolamide (DHEA or synaptamide), another NAE, demonstrates synaptogenic properties in the brain (11) and may reduce inflammation and pain (12–17). DHEA and other NAEs, such as palmitoylethanolamide (PEA) and oleoylethanolamide (OEA), are known to elevate PPAR transcriptional activity (18–20) and an increase in PPAR activity is one potential mechanism to explain their influence on neurological function. The DHEA precursor, DHA (22:6n-3), can be exogenously consumed from marine and seafood sources or endogenously synthesized from α -linolenic acid (18:3n-3) or other precursors within the n-3 PUFA biosynthesis pathway (21). One of these precursors, tetracosahexaenoic acid (THA, 24:6n-3), was first identified as an unstable precursor to DHA in 1991 (22), but was later determined to also be a product of DHA (23, 24). Compared with other n-3 PUFAs, THA is present at low levels in various tissues and blood (23, 25–27) but appears to be higher in the brain (25, 27). The low levels of THA appear due to a short half-life and rapid turnover (23) and may suggest an important role for THA in various tissues for the rapid conversion to metabolites important in biological functions. Previously, we demonstrated that unesterified DHA and ARA

This article contains [supplemental data](#).

[†]These authors should be considered co-first authors.

*For correspondence: Adam H. Metherel, adam.metherel@utoronto.ca

were increased in mouse brain during periods of ischemia/hypercapnia (28), and that this elevation was exacerbated in FAAH-KO mice. Furthermore, DHEA was increased in ischemic/hypercapnic wild-type and FAAH-KO mice, with FAAH-KO mice exhibiting up to four times higher levels of DHEA in the brain compared with wild-type mice (28).

To the best of our knowledge, a THA-derived tetracosahexaenoylethanolamide (THEA) has not been characterized and may be a bioactive mediator. In our study, we chemically synthesized THEA as an authentic standard and developed a LC-MS/MS method to measure levels of THEA in vivo. Furthermore, we examined how ischemia/hypercapnia and deletion of the FAAH enzyme affected THEA and THA levels in the mouse brain, and then assessed the effects of THEA on neurotransmission by evaluating the response of accumbal γ aminobutyric acid (GABA)ergic MSN to THEA exposure. We observed increased neuronal output in response to THEA exposure, suggesting a role for THEA in regulating neuronal excitability.

MATERIALS AND METHODS

Organic synthesis of DHEA and THEA

Methods for DHEA and THEA synthesis were adopted from Karaulov et al. (29). Briefly, DHA (Nu-Chek Prep, Inc., Elysian, MN) and THA methyl esters (Larodan, Inc., Monroe, MI) were treated with fresh monoethanolamine (1:5 molar ratio; Millipore-Sigma, Burlington, MA) and trifluoroacetic acid (Millipore-Sigma). The mixture was vortexed and heated at 140°C for 1 h, cooled to room temperature, and extracted with chloroform. Following addition of chloroform, the mixture was acidified by adding 10% aqueous HCl to a pH of 3, allowing for the formation of monoethanolamine salts that could be then be separated in the aqueous phase from the THEA-containing chloroform layer. The lower chloroform layer was removed and the chloroform + HCl extraction was repeated. The combined chloroform fractions were evaporated under a stream of nitrogen. The NAEs (DHEA or THEA) were further isolated by TLC and dissolved in ethanol for further analysis.

Separation and purification of THEA using HPLC

THEA separation and identification was performed using HPLC (Waters 2690, Boston, MA) with a Luna C18 reverse-phase column (4.6 × 250 mm, 100 Å; Phenomenex, Torrance, CA) equipped with an in-line UV photodiode array detector (Waters 996), which monitors a wavelength of 242 nm. Briefly, solvent (A) (100% water) and solvent (B) (100% acetonitrile) were used at a 1 ml/min gradient system, an isocratic mobile phase condition of 95% (B) for 20 min and injection volume of 50 μ l. All fractions were collected at 1 min intervals for a total of 20 min and then analyzed by liquid scintillation counting.

Identification and quantification of THEA using HPLC-MS

MS/MS was performed with a SCIEX QTrap5500 mass spectrometer (SCIEX, Framingham, MA) with an Agilent 1290 HPLC system (Agilent Technologies, Santa Clara, CA) equipped with a Phenomenex Kinetex XB-C18 column, 50.9 × 4.6 mm, 2.6 μ m (Phenomenex) and set to a flow rate of 600 μ l/min (28). The ion mass transitions used were as follows: DHEA (m/z 372.3/62.0), DHEA-d4 (m/z 376.3/66.0), THEA (m/z 400.3/62). Peak integration and data analysis were performed using Analyst® software (SCIEX).

Animals

Animal experiments for FAAH-KO studies were performed in accordance with relevant guidelines and regulations of the Animal Care Committee of the University of Toronto (#20011517). FAAH-KO mice were obtained from Dr. Ben Cravatt, Department of Chemistry at Scripps Research Institute (La Jolla, CA). Brain samples were obtained from FAAH-KO and C57BL/6J wild-type mice as secondary analysis of our previously published study (28). Mice were housed in groups of four per cage with a 12:12 h light:dark cycle in a temperature-controlled (21°C) and humidity-controlled (40%) environment, with ad libitum access to standard chow and water. At 12 weeks of age, animals were fasted for 12 h prior to euthanization. The animals ($n = 8-9$ per group) were randomly assigned to one of three euthanasia groups: *i*) head-focused, high energy microwave irradiation (microwave; 1 kW, 0.88–0.99 s; Cober Electronics Inc., Stratford, CT); *ii*) CO₂ + microwave (5 min CO₂ then microwave fixation); or *iii*) CO₂ only (CO₂ 5 min only). Whole brain required approximately 5 min per animal for removal, after which the brains were immediately stored at –80°C until further analysis.

Animal experiments for ex vivo whole-cell patch electrophysiology were conducted in accordance with the European directive 2010/63/UE and approved by the French Ministry of Research and the local ethics committee (CEEA Bordeaux N°55; APAFIS #50150171-A). Wild-type C57BL/6J mice were housed 8–10 per cage with a 12:12 h light:dark cycle in a temperature-controlled (23 ± 1°C) and humidity-controlled (40%) environment, with ad libitum access to standard chow and water. All experiments were conducted in compliance with ARRIVE guidelines.

Whole brain total THA extraction and GC-MS

Total lipid extracts (TLEs) were obtained from frozen powdered whole brain samples according to a modified Folch method (30) and similarly to previous studies performed in our laboratory (28). Briefly, lipids were extracted with 2:1 chloroform:methanol containing a known amount of ²H₈ (deuterated-6-8, D8)-arachidonic acid (20:4n-6) (Cambridge Isotope Laboratories, Inc., Tewksbury, MA) as an internal standard to determine THA concentration. The mixtures were vortexed, and 0.88% potassium chloride was added to separate solvent phases. The samples were then centrifuged at 500 *g* for 10 min, and the lower lipid-containing chloroform layer was transferred to a new test tube and stored at –80°C. The TLE was aliquoted for separate total fatty acid and unesterified fatty acid analysis, as previously described (31). Briefly, for total fatty acids, the TLE portion was saponified with 10% potassium hydroxide in methanol (w:v), and the unesterified fatty acids were isolated by TLC with 60:40:2 (v:v:v) heptane:diethyl ether:acetic acid, bands scraped, and extracted with 2:1 chloroform:methanol. Following this, saponified total fatty acids and isolated unesterified fatty acids were converted to pentafluorobenzyl esters by heating at 60°C in 1:10:1,000 (v:v:v) pentafluorobenzyl bromide:diisopropylamine:acetonitrile (32), dried under nitrogen gas, and dissolved in 100 μ l of hexane for GC-MS analysis. Total THA and unesterified THA were analyzed on an Agilent 5977A quadrupole mass spectrometer coupled to an Agilent 7890B gas chromatograph (Agilent Technologies, Mississauga, ON, Canada) in negative chemical ionization mode. The details of the GC-MS set up were described previously (28, 32). In this study, THA was analyzed in selected ion monitoring mode using M-1 for parent ion identification with ion dwell times of 500 ms. The parent ion mass ($M - H^+$) for THA is 355.3.

THEA extraction in brain samples

THEA was extracted from powdered brain samples (28, 33). Briefly, samples were mixed with the 50 μ l of DHEA-D4 (Cayman Chemical Co., Ann Arbor, MI; 50 ng/ml) as an internal standard. The mixture was prepared with ice-cold acetone, homogenized, and

centrifuged. The supernatant was transferred into a clean tube and dried under nitrogen gas. Chloroform:methanol:deionized water (2:1:1, v:v:v) was then added to the dried samples, vortexed, and centrifuged at 500 *g* for 10 min at 4°C. The chloroform layer was transferred into another clean tube, dried under nitrogen gas, and dissolved in 100 μ l of acetonitrile. Finally, samples were transferred into vials for LC-MS/MS analysis. THEA was identified by LC-MS/MS; as described earlier, THEA concentrations were determined using the DHEA-D4 as the internal standard.

Transient transfection assay

HEK293 cells were cultured in high-glucose DMEM (Sigma, Oakville, ON) containing 10% FBS and 1% penicillin/streptomycin at 37°C in 5% CO₂. For transfection assays, cells were plated into a clear bottom white 96-well plate at a density of 40,000 cells per well in DMEM supplemented with 10% charcoal-stripped FBS (Invitrogen, Carlsbad, CA). The next day, cells were transfected with 150 ng/well of plasmid DNA mix (50 ng UAS-luciferase reporter, 20 ng β -galactosidase, 15 ng human nuclear receptor GAL4-PPAR and 65 ng of pGEM filler plasmid) using calcium phosphate. Six hours after transfection, cells were treated with vehicle (DMSO), varying concentrations of THEA (including 10, 25, and 50 μ M), endogenous fatty acid amide ligands or synthetic ligands as positive controls. All positive controls were purchased from Cayman Chemicals (Ann Arbor, MI). Endogenous fatty acid amide ligands were 25 μ M OEA and 25 μ M PEA. Synthetic ligands were 10 μ M WY14643 for PPAR α , 25 μ M rosiglitazone for PPAR γ , and 100 nM GW0742 for PPAR β/δ . The concentration of DMSO was held constant for all conditions at 0.1% (v/v). After 14–16 h of ligand treatment to allow for complete luciferase translation and accumulation, cells were harvested and assayed for luciferase and β -galactosidase activity. Luciferase values were corrected to the corresponding β -galactosidase values to control for transfection efficiency and expressed as relative luciferase units. The plasmids were a kind gift from Dr. David Mangelsdorf (University of Texas Southwestern Medical Centre, Dallas, TX).

Ex vivo whole-cell patch clamp electrophysiology

Animals were anesthetized using isoflurane (4–5%). After rapid decapitation, sagittal slices were cut using a VT1000S vibratome (Leica, Germany) at a thickness of 350 μ m in ice-cold oxygenated artificial cerebrospinal fluid (ACSF), containing: 125 mM NaCl, 2.5 mM KCl, 1.25 mM NaH₂PO₄, 2.0 mM CaCl₂, 1.0 mM MgCl₂, 25 mM NaHCO₃, 25 mM D-glucose, and 10 μ M pyruvic acid, pH 7.4, osmolality 310 mOsm. Slices were then equilibrated at 33.5 \pm 0.1°C for 60 min before returning to room temperature. During recording, slices were continuously perfused at 1–1.5 ml/min with oxygenated buffer at 30°C. Borosilicate pipettes (5–6 M Ω , 1.5 mm OD; Sutter Instrument) were filled with an intracellular solution containing: 128 mM K-gluconate, 20 mM NaCl, 1 mM MgCl₂, 1 mM EGTA, 0.3 mM CaCl₂, 2 mM Na₂-ATP, 0.3 mM Na-GTP, 0.2 mM cAMP, 10 mM HEPES; 290–300 mOsm, pH 7.3–7.4. Pipette offset was adjusted before each recording. MSNs of the nucleus accumbens core were visualized under direct interference contrast with 40 \times water immersion objective combined with an infra-red filter mounted on an upright BX51WI microscope (Olympus, France). Recordings were acquired using Multiclamp700B and Digidata 1440A (Axon Instrument, Molecular Devices). Current over voltage (I/V) curves were acquired in current-clamp mode without holding (I = 0). To evoke excitatory postsynaptic currents (EPSCs) at 0.1 Hz, a concentric bipolar electrode (Phymep, France) was placed on afferent glutamatergic fibers, recorded in MSNs under voltage-clamp configuration, with membrane potentials maintained at –70 mV. Spontaneous EPSCs were recorded during 1 min under voltage-clamp configuration with membrane potentials held at –70 mV. To perform excitation-spike (E-S)

coupling experiments, membrane potentials were held at –60 mV under current-clamp configuration with stimulations at 0.2 Hz. All data were sampled at 20 kHz and filtered at 1 kHz. Following 10 min of baseline recording, either THEA (100 nM prepared in ACSF from concentrated stock THEA in ethanol) or vehicle [0.02% (v:v) ethanol in ACSF] were applied over a 20 min period, with measurements performed 20 min after THEA or vehicle washout. Only data from putative GABAergic MSN were included in the present study and identified immediately after rupture of the G Ω seal by evaluating their responses to the injection of depolarizing currents, and is consistent with previous findings (34–36).

Statistics

All statistical analyses for THA and THEA were performed with GraphPad Prism 8.0.1. D'Agostino and Pearson omnibus normality tests for normality were conducted, and non-normally distributed data were log transformed prior to statistical analyses. Differences in total THA and unesterified THA concentrations were assessed by two-way ANOVA (genotype \times euthanasia method) followed by Tukey's multiple comparisons post hoc test. Due to the large differences in THEA levels between wild-type and FAAH-KO mice, any real differences due to methods of euthanasia become lost with a two-way ANOVA model; therefore, one-way ANOVAs with Tukey's multiple comparisons post hoc test to compare the effects of euthanasia methods within a genotype was performed for THEA. For the transient transfection assay, a one-way ANOVA followed by the Holm-Sidak test was performed for multiple comparisons against vehicle control group.

For electrophysiological experiments, all measurements were performed offline using Clampfit (Molecular Devices). For E-S coupling, the firing probability of a given neuron was plotted according to the EPSP slope, based on a previously published study (37). EPSP slopes were measured during the first 2.5 ms and spike probability was determined by establishing a survival curve where, for each measured slope, a spike was considered as an event. Significant differences in neuronal output were determined by the Log-rank (Mantel-Cox) test. Statistical significance was set as $P < 0.05$ for all analyses.

RESULTS

Verification of purity and identity of the synthesized DHEA and THEA

First, DHEA was synthesized and HPLC used to confirm the presence of the DHEA product and reagents (Fig. 1A) and compared with reference materials for commercially available reference standards of DHEA (Fig. 1B), DHA methyl ester (Fig. 1C), ethanolamine (reaction reagents) (Fig. 1D), and ethanol (reaction by-product) (Fig. 1E). The purified DHEA contained no traces of ethanolamine (Fig. 1D) or ethanol (Fig. 1E) but did contain trace amounts of DHA methyl ester (Fig. 1A). Therefore, we separated the synthesized DHEA from DHA ethyl ester by HPLC retention time.

THEA was then synthesized using THA methyl ester, and after checking for ethanolamine, THA methyl ester, and ethanol impurities, THEA was isolated and the purity confirmed by HPLC (Fig. 2A). The identity of the THEA was further confirmed by LC-MS/MS with mass transitions of m/z 400.3 and 61.9, representing the THEA parent ion and ethanolamine daughter ion, respectively (Fig. 2B).

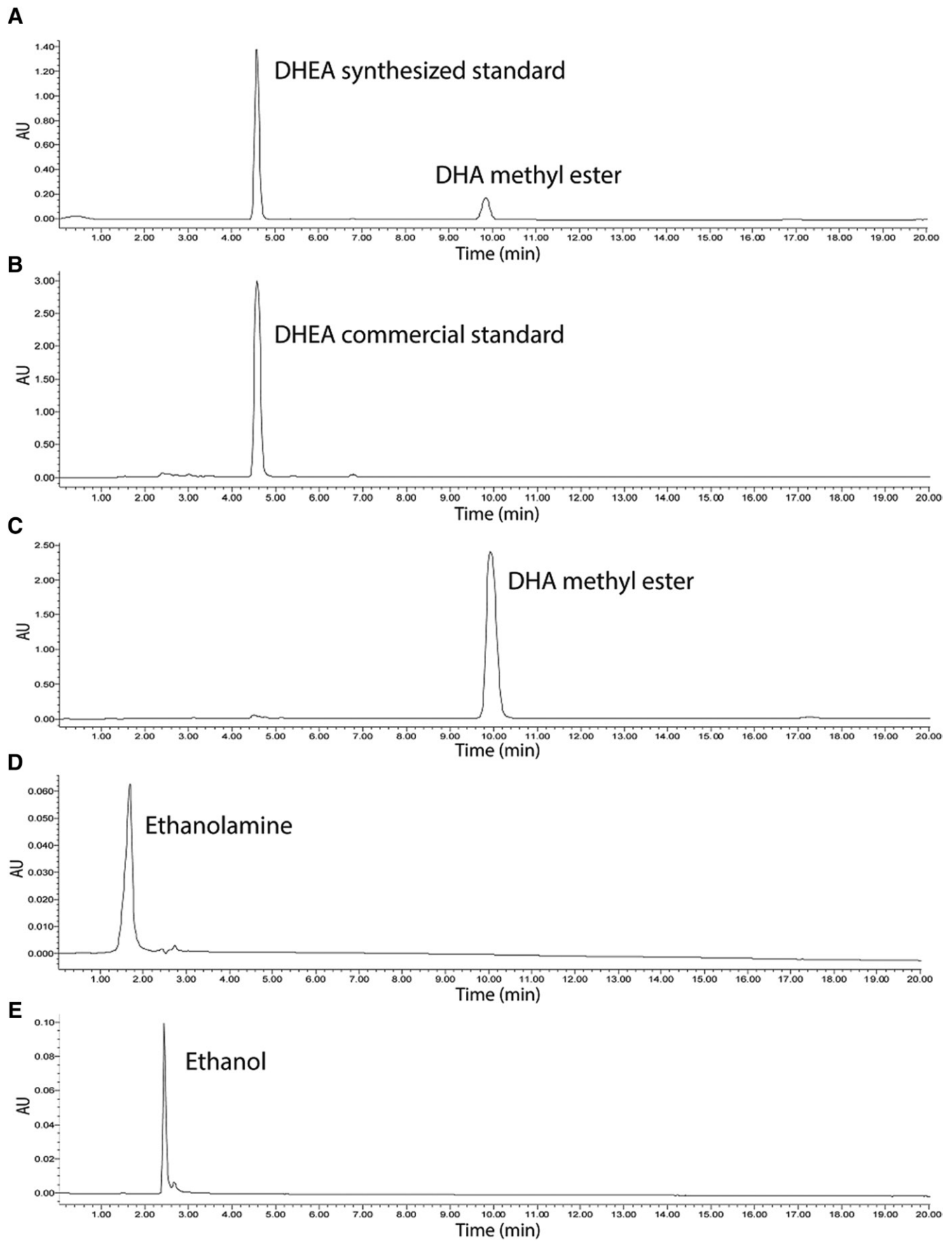


Fig. 1. Representative HPLC chromatograms of DHEA and contaminants. Chromatograms of laboratory synthesized DHEA (A) compared with chromatograms for reference standards of commercially available DHEA (B), DHA methyl ester (C), ethanolamine (D), and ethanol (E).

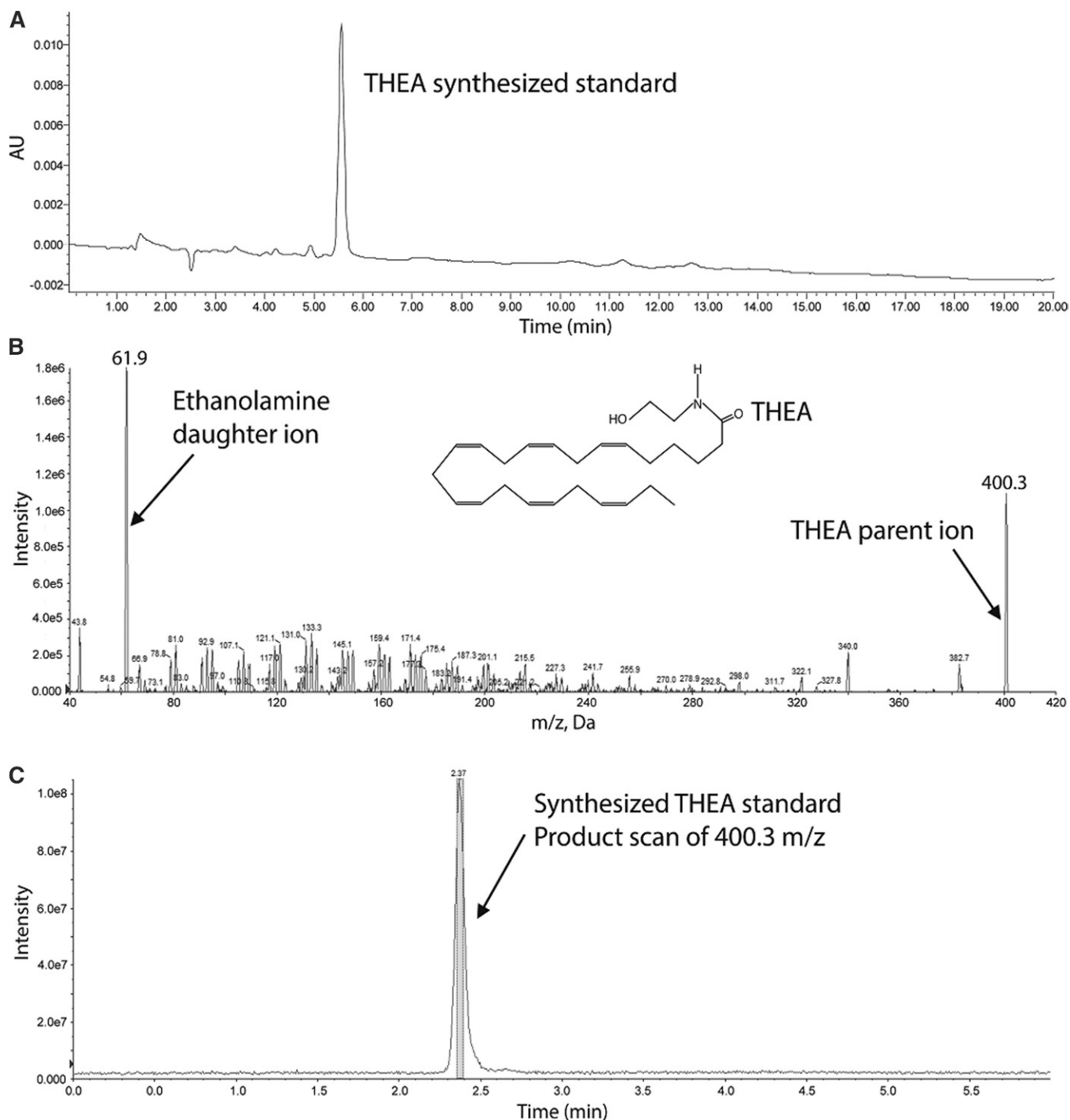


Fig. 2. Representative chromatograms and mass spectra of organically synthesized THEA following purification. HPLC chromatogram of synthesized and purified THEA (A), LC-MS/MS mass spectra of synthesized THEA (B), and LC-MS/MS chromatogram of synthesized THEA (C).

Mass transitions and retention time of our synthesized THEA standard (Fig. 2C) were used to accurately identify THEA in whole-brain samples from the mice.

CO₂-induced ischemia/hypercapnia on whole-brain THA, unesterified THA, and THEA

There was an interaction effect between genotype and euthanasia method on unesterified THA levels (Fig. 3A). The interaction effect showed that microwave fixation significantly prevented the elevation of unesterified THA during

ischemia/hypercapnia in both FAAH-KO and wild-type mice. CO₂-induced ischemia/hypercapnia elevated unesterified THA levels in a step-up pattern as microwave < CO₂ + microwave < CO₂ only in both genotypes. In addition, FAAH-KO mice in the CO₂-only group had higher levels of unesterified THA compared with any other groups. FAAH-KO mice also had higher unesterified brain THA in the CO₂ + microwave and CO₂-only groups compared with wild-type mice. Total brain THA levels were not significantly affected by FAAH genotype or euthanasia method ($P > 0.05$, Fig. 3B).

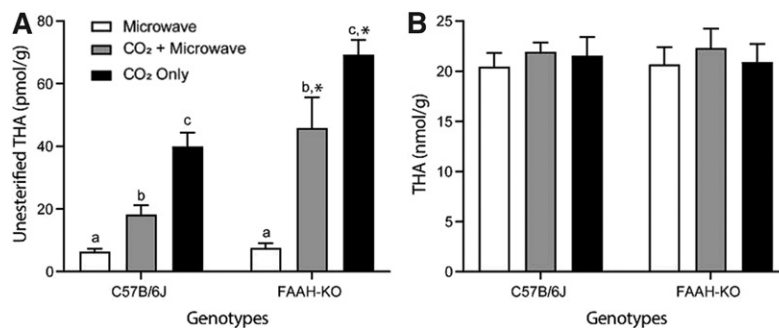


Fig. 3. Ischemia/hypercapnia and FAAH-KO increases brain unesterified THA. Whole-brain concentrations of unesterified THA (A) and total THA (B) in wild-type (C57B/6J) and FAAH-KO mice following euthanasia by either head-focused microwave fixation (microwave), carbon dioxide (CO₂) asphyxiation followed immediately by microwave (CO₂ + microwave), or CO₂ only. Different letters represent statistically different values between euthanasia method within genotype, and asterisks (*) represent statistically significant differences between genotype within a euthanasia method following two-way ANOVA (genotype × euthanasia method), $P < 0.05$. Following significant interaction effects, one-way ANOVAs followed by Tukey's post hoc test were performed to compare the effect of euthanasia method within genotype, and *t*-tests were performed comparing genotype within a euthanasia method, $P < 0.05$. Values are expressed as mean ± SEM, $n = 8$ –9 per group.

In the C57B/6J mice, both CO₂ + microwave and CO₂-only groups had higher THEA levels compared with the microwave group ($P = 0.0226$) (Fig. 4A). Although the levels of THEA were significantly higher in the FAAH-KO mice compared with the C57B/6J mice, CO₂-induced ischemia/hypercapnia did not affect the levels of THEA in the FAAH-KO mice (Fig. 4A), and this is further depicted with representative chromatograms of THEA from the CO₂-only groups of the wild-type (Fig. 4B) and the FAAH-KO mice (Fig. 4C). Importantly, THEA could only be detected in two mice from each of the microwave and CO₂ + microwave groups, suggesting even lower brain THEA levels than we are reporting.

THEA does not activate the PPARs

OEA and PEA are long-chain fatty acid amides that have previously been shown to activate PPAR α (both) or PPAR β/δ (OEA only) (18, 19). To assess whether THEA would also have activity at these receptors, we performed a transient transfection assay in HEK293 cells. The synthetic PPAR agonists, WY14643, rosiglitazone, and GW0742, strongly activated human PPAR α , PPAR γ , and PPAR β/δ , respectively, demonstrating the functionality of the assay (Fig. 5). OEA and PEA induced the activity of PPAR α (Fig. 5A), and OEA also weakly activated PPAR β/δ (Fig. 5C) while showing no activity toward PPAR γ (Fig. 5B). In contrast, PEA had no agonist effects on PPAR γ or PPAR β/δ (Fig. 5B, C), consistent with previous studies (18, 19). THEA was tested at 10, 25, and 50 μ M, and showed no activity toward any of the PPAR isoforms (Fig. 5).

THEA increases neuronal output of accumbal MSNs

Using whole-cell patch clamp electrophysiology on sagittal slices, we recorded MSNs in the nucleus accumbens core (supplemental Fig. S1A). Compared with control conditions (ethanol 0.02% v/v), we found no effect of THEA exposure (100 nM during 20 min) on the intrinsic electrophysiological properties of MSNs, including resting membrane potential, input resistance, and cell capacitance

(supplemental Fig. S1B–D), or action potential properties, such as action potential threshold, amplitude, and duration (supplemental Fig. S1E–H). THEA did not alter either passive membrane potential (supplemental Fig. S1I, J) or the number of spikes (supplemental Fig. S1K) in response to current injections. However, THEA exposure significantly increased the firing probability for a given neuron following afferent glutamatergic fiber stimulation ($\chi^2 = 15.27$, Log-rank Mantel-Cox test, $P < 0.0001$; Fig. 6A–C), indicating increased excitability in these neurons. Indeed, while 50% spike probability was achieved at 6.1 mV/ms in control conditions, 4.9 mV/ms was sufficient after THEA exposure, denoting increased neuronal output.

DISCUSSION

To our knowledge, this is the first study to measure THEA and assess its function. As there was no commercially available reference standard of THEA, we first confirmed that any signal obtained by MS was not the result of a molecule of identical mass and retention time. Therefore, it was necessary to synthesize a THEA standard from accepted methodologies (29). Importantly, we first assessed our synthesis protocol for DHEA so that we could compare it to a commercially available DHEA standard and were then able to synthesize and purify a THEA standard that could be used for accurate identification of THEA in mouse whole brain. Overall, results from whole brain of mice identified the presence of a novel NAE, THEA, in the brains of mice.

Whole-brain THEA levels were higher during ischemic/hypercapnic conditions (CO₂ + microwave and CO₂-only euthanasia methods) compared with the nonischemic (microwave only) condition in the wild-type mice. This is similar to what we observed previously for DHEA, OEA, and AEA (28). Furthermore, THEA levels were 15- to 20-fold higher in the FAAH-KO mice compared with wild-type mice with no effect of the ischemia/hypercapnia in the

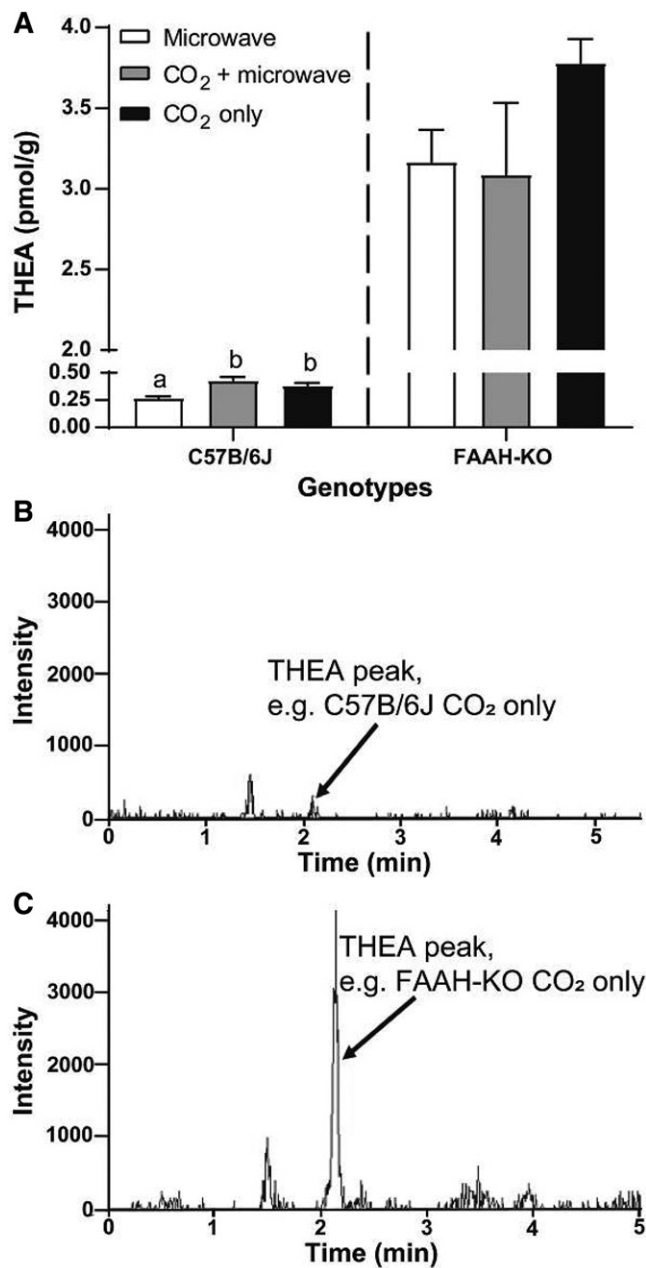


Fig. 4. Ischemia/hypercapnia and FAAH-KO increase brain THEA. **A:** Whole brain concentrations of THEA in wild-type (C57B/6J) and FAAH-KO mice following euthanasia by either head-focused microwave fixation (microwave), carbon dioxide (CO₂) asphyxiation followed immediately by microwave (CO₂ + microwave), or CO₂ only. Different letters represent statistically different values between euthanasia method within genotype by one-way ANOVA (genotype × euthanasia method) followed by Tukey's post hoc test, $P < 0.05$. Values are expressed as mean ± SEM, $n = 8-9$ per group, except C57B/6J mice of microwave and CO₂ + microwave groups ($n = 2$) due to THEA being below the limit of detection in six to seven samples per group (see the Discussion for more details). LC-MS/MS chromatogram of whole-brain THEA from wild-type CO₂-only mouse (**B**) and LC-MS/MS chromatogram of whole-brain THEA from FAAH-KO CO₂-only mouse (**C**).

FAAH-KO animals. The elevated THEA in FAAH-KO matches very closely with our previous findings and suggests that THEA is catabolized by FAAH similarly to other

NAEs (28). The lack of any further increase in THEA levels in the ischemic/hypercapnic FAAH-KO mice suggests a potential limit or ceiling for brain THEA levels. Although we can confidently quantify the levels of THEA in ischemic/hypercapnic wild-type mice when euthanized by the CO₂-only method, THEA was only detectable in two nonischemic mice (microwave method) and two partially ischemic mice (CO₂ + microwave), and may limit some of our interpretations. Nevertheless, by reporting the mean of the detected samples, this leads to an overestimation of the true values, which in turn leads to an underestimation of the effect of ischemia/hypercapnia on THEA levels. Therefore, our broad interpretation that ischemia/hypercapnia leads to an increase in brain THEA levels remains intact.

We showed no measurable change in the levels of total-brain THA; however, unesterified THA levels increase upon ischemia/hypercapnia as shown previously with other fatty acids (28, 38), and this response appears to be exacerbated in the FAAH-KO mice. Unlike our previous findings where the increases in unesterified brain DHA was accompanied by similar increases in DHEA with ischemia/hypercapnia in the FAAH-KO animals (28), the increase in unesterified THA levels was not matched by a concomitant increase in THEA. This suggests a saturation in THEA synthesis, despite continued increases in the unesterified THA precursor, resulting from limitations in either the activity or level of the THEA-synthesizing process, and possibly *N*-acylphosphatidylethanolamine phospholipase D (39). Nevertheless, other enzymes capable of synthesizing or metabolizing NAEs, including monoacylglyceride lipase, acid ceramidase, and *N*-acylethanolamine-hydrolyzing acid amidase, may be differentially activated or regulated in the FAAH-KO model; thus, additional studies are warranted to test these possible interactions in FAAH-KO mice.

It is also possible that a rapid conversion of THA to THEA is met (and exceeded under normal baseline conditions) by a similarly rapid metabolic consumption of THEA. Such a rapid metabolism of THEA is highlighted by our inability to identify the molecule above our limits of detection in all but two of the animals per microwave euthanasia group, and such rapid consumption by neural tissues indicates an important role for THEA in healthy neurological functioning. Future studies may be designed using intracerebroventricular injections of THEA to determine the half-life in the brain compared with other NAEs, such as DHEA. Alternatively, THA is rapidly converted to DHA *in vivo* (23), and if THEA synthesis is saturated, the excess unesterified THA in the brain could be used to synthesize additional DHA, and in turn DHEA. These are important molecules in neuroinflammation, as both unesterified DHA (40) and DHEA (41) are protective against lipopolysaccharide-induced neuroinflammation in rodent models.

Relative to the blood and other tissues, the brain has some of the highest levels of THA in the body (23, 25-27), and may therefore have added importance in neural tissues. In our animals, total brain THA was at least 20 nmol/g across all conditions and is substantially higher than previous reports of 1-6 nmol/ml THA in rodent plasma (23, 26) and 1-3 nmol/ml in human plasma (42). This enrichment

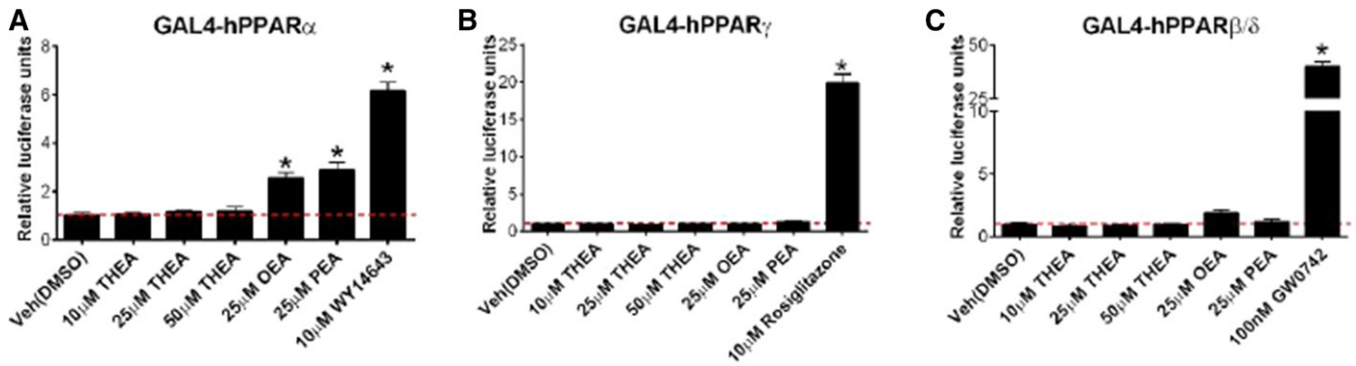


Fig. 5. THEA does not activate PPAR α , PPAR β/δ , or PPAR γ in a cotransfection assay. HEK293 cells were transfected with GAL4-hPPAR α , GAL4-hPPAR γ , or GAL4-hPPAR β/δ and UAS-luciferase reporter plasmid. The values were normalized to vehicle control (DMSO). * $P < 0.05$ versus vehicle (Veh) (DMSO); one-way ANOVA followed by Holm-Sidak test. The dashed line was set to 1 for ease of comparison. OEA, PEA, WY14643, rosiglitazone, and GA0742 were used as positive controls. Values are expressed as mean \pm SD, $n = 3$ per group.

in brain THA could be due to either a higher rate of uptake into the brain or an increase in synthesis from n-3 PUFA precursors such as EPA (20:5n-3) and/or DHA (23, 31). To this point, cell lines originating from neural tissues, neuroblastoma (SK-N-SH) cells, and retinoblastoma (Y79) cells demonstrate strikingly different metabolism of DHA compared with cells originating from nonneural tissues, hepatocarcinoma (HepG2) cells, and breast cancer (MCF7) cells (24). Specifically, when incubated with ^{13}C -DHA over 24 h, neural tissues preferred elongation of DHA to THA instead of the retroconversion/ β -oxidation to the EPA pathway that appears to dominate in the nonneural tissues. This may support the hypothesis for a heightened demand for THA in neural tissues and the brain, possibly as a pool for THEA synthesis.

PEA and OEA are known activators of PPAR α (18, 19); OEA weakly activates PPAR β/γ , and the n-3 PUFA-derived eicosapentaenoylethanolamide and DHEA have been shown activate PPAR γ in MCF7 cells (20). Furthermore, PPAR α is not only activated in the brains of FAAH-KO mice (43), but

a reversal of drug-induced inhibition of MSN excitability has previously been shown to involve PPAR α activation without CBI involvement (44). In addition, it has been reported that through PPAR α activation, the resultant increase in neurosteroids may then act on GABA receptors (45) that are highly abundant in MSNs (46). With the understanding that multiple NAEs activate PPARs, we sought to determine whether THEA would also show activity toward the PPARs. Although we confirmed the activity of PEA and OEA toward PPAR α along with positive controls for PPAR α , PPAR γ , and PPAR β/δ , THEA showed no additional activity toward any of the PPARs in comparison to the vehicle.

MSNs represent the major neuronal population within the nucleus accumbens of the neostriatum (10). In our study, we assessed the effects of THEA on neuronal functioning in the MSNs of the nucleus accumbens and observed increased neuronal output following THEA exposure, indicating that THEA can modulate the extrinsic excitability of these neurons. This increase in neuronal output of accumbal MSNs

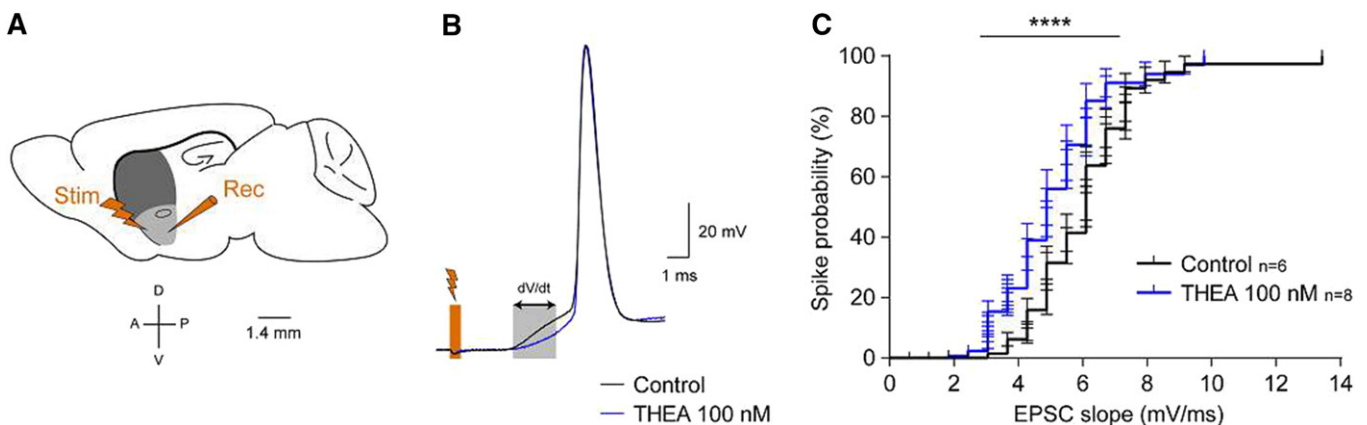


Fig. 6. THEA increases neuronal output of accumbal MSNs. (A) Representative drawing of a sagittal brain section in mice, with location of both glutamatergic fiber stimulation and MSN patch clamp recording. Dark gray, dorsal striatum; light gray, nucleus accumbens; A, anterior; P, posterior; D, dorsal; V, ventral. B: Typical electrophysiological E-S coupling experiment where stimulations of afferent glutamatergic fibers evoke spiking in the recorded neurons. The depicted traces represent two typical recordings following 0.02% ethanol (control) or 100 nM THEA exposures. The orange rectangle indicates stimulation occurrence, while the gray rectangle corresponds to the first 2.5 ms of neuronal responses where EPSC slopes (dV/dt) are measured. C: Significantly increased spike probability to stimulation in MSNs following THEA exposures (100 nM over 20 min), denoting increased excitability in these neurons. **** $P < 0.0001$ [Log-rank (Mantel-Cox) test]; n values represent sample number.

appears to occur without altering intrinsic electrophysiological properties. Such an increase in neuronal excitability can directly modulate dopamine-dependent functions, such as motivation. Here, we found that THEA enhanced synaptic integration in accumbal MSNs. Ischemic conditions are known to increase the excitability of striatal neurons (47–51), and the neostriatum has been considered as one of the brain regions most susceptible to ischemia. Furthermore, it has been shown that neurotransmission is affected by ischemia through metabolites derived from linoleic acid (52), a PUFA from the n-6 family. Collectively, the increase in THA-derived THEA following ischemia/hypercapnia and the ability of THEA to increase neuronal excitability suggests an important role for THEA during ischemia, particularly in the neostriatum. We therefore hypothesize that THEA can be implicated in neuromodulation during (or following) ischemic episodes in the brain. Furthermore, modes of increasing brain THA levels, possibly through diet (53), may be a means to further protect against ischemic episodes. With MSNs primarily being GABAergic in nature, future mechanistic studies might be designed to assess the effects of THEA on GABA receptors and GABAergic neurotransmission. Additional studies should assess whether THEA can modulate the activity of GABA neurons in other brain areas, and whether such effects are specific to GABA neuromodulation.

Current research on fatty acid and lipid metabolism involving THA and THEA is limited, with ours the first to ever report THEA. Our study has identified the presence of this novel endocannabinoid in mouse brain, its increase in ischemic/hypercapnic and FAAH-KO mice, and its ability to increase neuronal output in MSNs. However, the mechanisms by which these changes occur are not clear and warrant further investigation. In conclusion, we have identified a novel NAE, THEA, which is mobilized during periods of ischemia/hypercapnia and when FAAH is absent, and that modulates the electrical activity of MSNs within the nucleus accumbens core, suggesting an important physiological role that could be a target for future studies aimed at improving neurological functioning.

Data availability

All data are contained within the article. 



Acknowledgments

The authors thank the researchers of the Analytical Facility for Bioactive Molecules, Hospital for Sick Children, Toronto, Canada for assistance with LC-MS/MS analysis. The authors wish to thank Julien Leroy, Marielle Levillain, and Gregory Artaxet for taking care of the animals at the NutriNeuro facility.

Author contributions

L.L., A.H.M., M.D.M., Z.L., C.S., X.F., C.L.C., S.L., and R.P.B. experiments-design; L.L., A.H.M., M.D.M., Z.L., C.S., X.F. experiments; L.L., A.H.M., M.D.M. data analysis; L.L., A.H.M. writing-original draft; C.C., S.L., R.P.B. materials; A.H.M., R.P.B. writing-review and editing. All authors read and approved the manuscript.

Author ORCIDs

Lin Lin  <https://orcid.org/0000-0003-4702-7190>; Carolyn L. Cummins  <https://orcid.org/0000-0001-7603-6577>

Abbreviations

ACSF, artificial cerebrospinal fluid; AEA, arachidonylethanolamide; DHEA, docosahexaenylethanolamide; EPSC, excitatory postsynaptic current; E-S, excitation-spike; FAAH, fatty acid amide hydrolase; GABA, γ aminobutyric acid; MSN, medium spiny neuron; NAE, N-acylethanolamine; OEA, oleylethanolamide; PEA, palmitoylethanolamide; THA, tetracosahexanoic acid; THEA, tetracosahexaenylethanolamide; TLE, total lipid extract.

Funding and additional information

This study was supported by the Natural Sciences and Engineering Research Council of Canada (NSERC) to R.P.B. L.L. was funded by NSERC. S.L., X.F., and M.D.M. were funded by Inrae, Fondation de France, and Nouvelle Région Aquitaine. M.D.M. was also funded by Fondation pour la Recherche Médicale.

Conflict of interest

R.P.B. has received research grants from Bunge Ltd., Arctic Nutrition, the Dairy Farmers of Canada, and Nestle Inc., as well as travel support from Mead Johnson and MS equipment and support from SCIEX. In addition, R.P.B. is on the executive board of the International Society for the Study of Fatty Acids and Lipids and held a meeting on behalf of Fatty Acids and Cell Signaling, both of which rely on corporate sponsorship. R.P.B. has given expert testimony in relation to supplements and the brain. R.P.B. also provides complimentary fatty acid analysis for farmers, food producers, and others involved in the food industry, some of whom provide free food samples. The other authors declare that they have no conflicts of interest with the contents of this article.

Manuscript received July 9, 2020, and in revised form August 14, 2020. Published, JLR Papers in Press, August 21, 2020, DOI 10.1194/jlr.RA120001024.

REFERENCES

1. Devane, W. A., L. Hanus, A. Breuer, R. G. Pertwee, L. A. Stevenson, G. Griffin, D. Gibson, A. Mandelbaum, A. Etinger, and R. Mechoulam. 1992. Isolation and structure of a brain constituent that binds to the cannabinoid receptor. *Science*. **258**: 1946–1949.
2. Porter, A. C., and C. C. Felder. 2001. The endocannabinoid nervous system: unique opportunities for therapeutic intervention. *Pharmacol. Ther.* **90**: 45–60.
3. Alger, B. E. 2004. Endocannabinoids: getting the message across. *Proc. Natl. Acad. Sci. USA*. **101**: 8512–8513.
4. Cravatt, B. F., and A. H. Lichtman. 2003. Fatty acid amide hydrolase: an emerging therapeutic target in the endocannabinoid system. *Curr. Opin. Chem. Biol.* **7**: 469–475.
5. Blancaflor, E. B., A. Kilaru, J. Keereetaweep, B. R. Khan, L. Faure, and K. D. Chapman. 2014. N-acylethanolamines: lipid metabolites with functions in plant growth and development. *Plant J.* **79**: 568–583.
6. LoVerme, J., G. La Rana, R. Russo, A. Calignano, and D. Piomelli. 2005. The search for the palmitoylethanolamide receptor. *Life Sci.* **77**: 1685–1698.
7. De Luca, M. A., V. Valentini, Z. Bimpisidis, F. Cacciapaglia, P. Caboni, and G. Di Chiara. 2014. Endocannabinoid 2-arachidonoylglycerol self-administration by Sprague-Dawley rats and stimulation of in vivo dopamine transmission in the nucleus accumbens shell. *Front. Psychiatry.* **5**: 140.

8. Solinas, M., Z. Justinova, S. R. Goldberg, and G. Tanda. 2006. Anandamide administration alone and after inhibition of fatty acid amide hydrolase (FAAH) increases dopamine levels in the nucleus accumbens shell in rats. *J. Neurochem.* **98**: 408–419.
9. Bergamini, G., H. Sigrist, B. Ferger, N. Singewald, E. Seifritz, and C. R. Pryce. 2016. Depletion of nucleus accumbens dopamine leads to impaired reward and aversion processing in mice: Relevance to motivation pathologies. *Neuropharmacology.* **109**: 306–319.
10. Graveland, G. A., and M. DiFiglia. 1985. The frequency and distribution of medium-sized neurons with indented nuclei in the primate and rodent neostriatum. *Brain Res.* **327**: 307–311.
11. Kim, H. Y., A. A. Spector, and Z. M. Xiong. 2011. A synaptogenic amide N-docosahexaenoylethanolamide promotes hippocampal development. *Prostaglandins Other Lipid Mediat.* **96**: 114–120.
12. Balvers, M. G., H. M. Wortelboer, R. F. Witkamp, and K. C. Verhoeckx. 2013. Liquid chromatography-tandem mass spectrometry analysis of free and esterified fatty acid N-acyl ethanolamines in plasma and blood cells. *Anal. Biochem.* **434**: 275–283.
13. Kim, J., M. E. Carlson, G. A. Kuchel, J. W. Newman, and B. A. Watkins. 2016. Dietary DHA reduces downstream endocannabinoid and inflammatory gene expression and epididymal fat mass while improving aspects of glucose use in muscle in C57BL/6J mice. *Int. J. Obes. (Lond.)* **40**: 129–137.
14. Liisberg, U., K. R. Fauske, O. Kuda, E. Fjaere, L. S. Myrnel, N. Norberg, L. Froyland, I. E. Graff, B. Liaset, K. Kristiansen, et al. 2016. Intake of a Western diet containing cod instead of pork alters fatty acid composition in tissue phospholipids and attenuates obesity and hepatic lipid accumulation in mice. *J. Nutr. Biochem.* **33**: 119–127.
15. Pu, S., P. Eck, D. J. A. Jenkins, P. W. Connelly, B. Lamarche, P. M. Kris-Etherton, S. G. West, X. R. Liu, and P. J. H. Jones. 2016. Interactions between dietary oil treatments and genetic variants modulate fatty acid ethanolamides in plasma and body weight composition. *Br. J. Nutr.* **115**: 1012–1023.
16. Ramsden, C. E., D. Zamora, A. Makriyannis, J. T. Wood, J. D. Mann, K. R. Fautot, B. A. MacIntosh, S. F. Majchrzak-Hong, J. R. Gross, A. B. Courville, et al. 2015. Diet-induced changes in n-3- and n-6-derived endocannabinoids and reductions in headache pain and psychological distress. *J. Pain.* **16**: 707–716.
17. Wood, J. T., J. S. Williams, L. Pandarinathan, D. R. Janero, C. J. Lammi-Keefe, and A. Makriyannis. 2010. Dietary docosahexaenoic acid supplementation alters select physiological endocannabinoid-system metabolites in brain and plasma. *J. Lipid Res.* **51**: 1416–1423.
18. Fu, J., S. Gaetani, F. Oveysi, J. Lo Verme, A. Serrano, F. R. de Fonseca, A. Rosengarth, H. Luecke, B. Di Giacomo, G. Tarzia, et al. 2003. Oleylethanolamide regulates feeding and body weight through activation of the nuclear receptor PPAR- α . *Nature.* **425**: 90–93.
19. Lo Verme, J., J. Fu, G. Astarita, G. La Rana, R. Russo, A. Calignano, and D. Piomelli. 2005. The nuclear receptor peroxisome proliferator-activated receptor- α mediates the anti-inflammatory actions of palmitoylethanolamide. *Mol. Pharmacol.* **67**: 15–19.
20. Rovito, D., C. Giordano, D. Vizza, P. Plastina, I. Barone, I. Casaburi, M. Lanzino, F. De Amicis, D. Sisci, L. Mauro, et al. 2013. Omega-3 PUFA ethanolamides DHEA and EPEA induce autophagy through PPAR γ activation in MCF-7 breast cancer cells. *J. Cell. Physiol.* **228**: 1314–1322.
21. Domenichiello, A. F., A. P. Kitson, and R. P. Bazinet. 2015. Is docosahexaenoic acid synthesis from alpha-linolenic acid sufficient to supply the adult brain? *Prog. Lipid Res.* **59**: 54–66.
22. Voss, A., M. Reinhart, S. Sankarappa, and H. Sprecher. 1991. The metabolism of 7,10,13,16,19-docosapentaenoic acid to 4,7,10,13,16,19-docosahexaenoic acid in rat liver is independent of a 4-desaturase. *J. Biol. Chem.* **266**: 19995–20000.
23. Metherel, A. H., R. J. S. Lacombe, R. Chouinard-Watkins, and R. P. Bazinet. 2019. Docosahexaenoic acid is both a product of and a precursor to tetracosahexaenoic acid in the rat. *J. Lipid Res.* **60**: 412–420.
24. Park, H. G., P. Lawrence, M. G. Engel, K. Kothapalli, and J. T. Brenna. 2016. Metabolic fate of docosahexaenoic acid (DHA; 22:6n-3) in human cells: direct retroconversion of DHA to eicosapentaenoic acid (20:5n-3) dominates over elongation to tetracosahexaenoic acid (24:6n-3). *FEBS Lett.* **590**: 3188–3194.
25. Lin, Y. H., S. Shah, and N. Salem, Jr. 2011. Altered essential fatty acid metabolism and composition in rat liver, plasma, heart and brain after microalgal DHA addition to the diet. *J. Nutr. Biochem.* **22**: 758–765.
26. Metherel, A. H., A. F. Domenichiello, A. P. Kitson, Y. H. Lin, and R. P. Bazinet. 2017. Serum n-3 tetracosapentaenoic acid and tetracosahexaenoic acid increase following higher dietary alpha-linolenic acid but not docosahexaenoic acid. *Lipids.* **52**: 167–172.
27. Pawlosky, R., A. Barnes, and N. Salem, Jr. 1994. Essential fatty acid metabolism in the feline: relationship between liver and brain production of long-chain polyunsaturated fatty acids. *J. Lipid Res.* **35**: 2032–2040.
28. Lin, L., A. H. Metherel, P. J. Jones, and R. P. Bazinet. 2017. Fatty acid amide hydrolase (FAAH) regulates hypercapnia/ischemia-induced increases in n-acylethanolamines in mouse brain. *J. Neurochem.* **142**: 662–671.
29. Karaulov, A. E., V. G. Rybin, D. V. Kuklev, and V. N. Akulin. 2004. Synthesis of fatty-acid ethanolamides from Linum catharticum oils and Cololabis saira fats. *Chem. Nat. Compd.* **40**: 222–226.
30. Folch, J., M. Lees, and G. H. Sloane Stanley. 1957. A simple method for the isolation and purification of total lipides from animal tissues. *J. Biol. Chem.* **226**: 497–509.
31. Metherel, A. H., R. J. S. Lacombe, J. J. Aristizabal Henao, D. Morin-Rivron, A. P. Kitson, K. E. Hopperton, D. Chalil, M. Masoodi, K. D. Stark, and R. P. Bazinet. 2018. Two weeks of docosahexaenoic acid (DHA) supplementation increases synthesis-secretion kinetics of n-3 polyunsaturated fatty acids compared to 8 weeks of DHA supplementation. *J. Nutr. Biochem.* **60**: 24–34.
32. Pawlosky, R. J., H. W. Sprecher, and N. Salem. 1992. High-sensitivity negative-ion GC-MS method for detection of desaturated and chain-elongated products of deuterated linoleic and linolenic acids. *J. Lipid Res.* **33**: 1711–1717.
33. Lin, L., H. Yang, and P. J. Jones. 2012. Quantitative analysis of multiple fatty acid ethanolamides using ultra-performance liquid chromatography-tandem mass spectrometry. *Prostaglandins Leukot. Essent. Fatty Acids.* **87**: 189–195.
34. Fino, E., J. Glowinski, and L. Venance. 2007. Effects of acute dopamine depletion on the electrophysiological properties of striatal neurons. *Neurosci. Res.* **58**: 305–316.
35. Gertler, T. S., C. S. Chan, and D. J. Surmeier. 2008. Dichotomous anatomical properties of adult striatal medium spiny neurons. *J. Neurosci.* **28**: 10814–10824.
36. Mao, M., A. Nair, and G. J. Augustine. 2019. A novel type of neuron within the dorsal striatum. *Front. Neural Circuits.* **13**: 32.
37. Campanac, E., and D. Debanne. 2008. Spike timing-dependent plasticity: a learning rule for dendritic integration in rat CA1 pyramidal neurons. *J. Physiol.* **586**: 779–793.
38. Deutsch, J., S. I. Rapoport, and A. D. Purdon. 1997. Relation between free fatty acid and acyl-CoA concentrations in rat brain following decapitation. *Neurochem. Res.* **22**: 759–765.
39. Lin, L., A. H. Metherel, A. P. Kitson, S. M. Alashmali, K. E. Hopperton, M. O. Trepanier, P. J. Jones, and R. P. Bazinet. 2018. Dietary fatty acids augment tissue levels of n-acylethanolamines in n-acylphosphatidylethanolamine phospholipase D (NAPE-PLD) knockout mice. *J. Nutr. Biochem.* **62**: 134–142.
40. Orr, S. K., S. Palumbo, F. Bosetti, H. T. Mount, J. X. Kang, C. E. Greenwood, D. W. Ma, C. N. Serhan, and R. P. Bazinet. 2013. Unesterified docosahexaenoic acid is protective in neuroinflammation. *J. Neurochem.* **127**: 378–393.
41. Park, T., H. Chen, K. Kevala, J. W. Lee, and H. Y. Kim. 2016. N-docosahexaenoylethanolamine ameliorates LPS-induced neuroinflammation via cAMP/PKA-dependent signaling. *J. Neuroinflammation.* **13**: 284.
42. Lin, Y. H., J. R. Hibbeln, A. F. Domenichiello, C. E. Ramsden, N. M. Salem, C. T. Chen, H. Jin, A. B. Courville, S. F. Majchrzak-Hong, S. I. Rapoport, et al. 2018. Quantitation of human whole-body synthesis-secretion rates of docosahexaenoic acid and eicosapentaenoic acid from circulating unesterified alpha-linolenic acid at steady state. *Lipids.* **53**: 547–558.
43. Mazzola, C., J. Medalie, M. Scherma, L. V. Panlilio, M. Solinas, G. Tanda, F. Drago, J. L. Cadet, S. R. Goldberg, and S. Yasar. 2009. Fatty acid amide hydrolase (FAAH) inhibition enhances memory acquisition through activation of PPAR- α nuclear receptors. *Learn. Mem.* **16**: 332–337.
44. Luchicchi, A., S. Lecca, S. Carta, G. Pillolla, A. L. Muntoni, S. Yasar, S. R. Goldberg, and M. Pistis. 2010. Effects of fatty acid amide hydrolase inhibition on neuronal responses to nicotine, cocaine and morphine in the nucleus accumbens shell and ventral tegmental area: involvement of PPAR- α nuclear receptors. *Addict. Biol.* **15**: 277–288.

45. Nisbett, K. E., and G. Pinna. 2018. Emerging therapeutic role of PPAR- α in cognition and emotions. *Front. Pharmacol.* **9**: 998.
46. Yager, L. M., A. F. Garcia, A. M. Wunsch, and S. M. Ferguson. 2015. The ins and outs of the striatum: role in drug addiction. *Neuroscience*. **301**: 529–541.
47. Arcangeli, S., A. Tozzi, M. Tantucci, C. Spaccatini, A. de Iure, C. Costa, M. Di Filippo, B. Picconi, C. Giampa, F. R. Fusco, et al. 2013. Ischemic-LTP in striatal spiny neurons of both direct and indirect pathway requires the activation of D1-like receptors and NO/soluble guanylate cyclase/cGMP transmission. *J. Cereb. Blood Flow Metab.* **33**: 278–286.
48. Armogida, M., M. Giustizieri, C. Zona, S. Piccirilli, R. Nistico, and N. B. Mercuri. 2010. N-ethyl lidocaine (QX-314) protects striatal neurons against ischemia: an in vitro electrophysiological study. *Synapse*. **64**: 161–168.
49. Calabresi, P., C. M. Ascone, D. Centonze, A. Pisani, G. Sancesario, V. D'Angelo, and G. Bernardi. 1997. Opposite membrane potential changes induced by glucose deprivation in striatal spiny neurons and in large aspiny interneurons. *J. Neurosci.* **17**: 1940–1949.
50. Calabresi, P., G. A. Marfia, D. Centonze, A. Pisani, and G. Bernardi. 1999. Sodium influx plays a major role in the membrane depolarization induced by oxygen and glucose deprivation in rat striatal spiny neurons. *Stroke*. **30**: 171–179.
51. Xu, Z. C. 1995. Neurophysiological changes of spiny neurons in rat neostriatum after transient forebrain ischemia: an in vivo intracellular recording and staining study. *Neuroscience*. **67**: 823–836.
52. Hennebelle, M., Z. Zhang, A. H. Metherel, A. P. Kitson, Y. Otoki, C. E. Richardson, J. Yang, K. S. S. Lee, B. D. Hammock, L. Zhang, et al. 2017. Linoleic acid participates in the response to ischemic brain injury through oxidized metabolites that regulate neurotransmission. *Sci. Rep.* **7**: 4342.
53. Gotoh, N., K. Nagao, H. Ishida, K. Nakamitsu, K. Yoshinaga, T. Nagai, F. Beppu, A. Yoshinaga-Kiriake, H. Watanabe, and T. Yanagita. 2018. Metabolism of natural highly unsaturated fatty acid, tetracosahexaenoic acid (24:6n-3), in C57BL/KsJ-db/db mice. *J. Oleo Sci.* **67**: 1597–1607.